Ocean Engineering 92 (2014) 162–174

Contents lists available at ScienceDirect

Ocean Engineering

journal homepage: www.elsevier.com/locate/oceaneng

Analysis of heave motions of a truss spar platform with semi-closed moon pool

Liqin Liu [a,b,*], Atilla Incecik [b], Yongheng Zhang [a], Yougang Tang [a]

[a] State Key Laboratory of Hydraulic Engineering Simulation and Safety Tianjin University, Tianjin 300072, China
[b] Department of Naval Architecture, Ocean and Marine Engineering, University of Strathclyde, Glasgow G4 0LZ, UK

ARTICLE INFO

Article history:
Received 29 April 2014
Accepted 7 September 2014
Available online 23 October 2014

Keywords:
Truss spar platform
Semi-closed moon pool
Heave motions
Dynamic coupling
Model experiments

ABSTRACT

This paper presents the heave motion of a truss Spar platform in regular waves considering the dynamic coupling between the motions of the platform and water in the moon pool. For a spar platform with semi-closed moon pool, water can flow freely through the guide plate at bottom of the moon pool. The mass of water inside the moon pool is comparable to the platform mass itself if the top tension riser system is used. Then the effect of the moon pool water on the motions of the platform should not be ignored. In the study presented in the paper, a 2-DOF (Degree of Freedom) dynamic coupling equations of the heave motions of the spar platform and the vertical motions of water in the moon pool were derived considering that the moon pool is totally closed, or 30% or 70% open. The results show that motions of water in the moon pool significantly affect the heave motions of the spar platform. Parametric study was also carried out to find the effect of the ratio of opening of the bottom plate on the coupled motions. Finally the model experiments were carried out to validate the numerical calculations.

1. Introduction

Spar platforms are one of the platform types used to produce oil and gas from deep-sea fields. Research investigations on Spar platforms mainly focus on wave loading on the hull and its hydrodynamic characteristics, the dynamic response of the platform, stability analysis of coupled heave and pitch motions, simulation of the mooring and the riser system and the vortex-induced vibration (Tang, 2008). Investigators so far have carried out extensive research on the coupled motions between the platform hull and its mooring and riser systems, as well as on the coupling effects of different degrees of freedoms (Kim et al., 2001; Tao et al., 2004; Mohammed et al., 2011; Xu and Jing, 2013). On the other hand the investigations to study the coupled motions between the platform and water inside the moon pool are rare.

Risers and drilling string go through a moon pool which is located in the centre of the hull of a spar platform and extends from the bottom of the hull to the deck. A guide plate is placed at the bottom of the moon pool (Drobyshevski, 2004; Kristiansen and Faltinsen, 2012). According to the design requirements, the moon pool is sometimes designed to be semi-closed, such as Holstein Spar platform, which allows water to flow freely in and out of the moon pool. There are two common ways to deal with the water inside a semi-closed moon pool (Gupta et al., 2008): (1) the moon pool is completely closed and the water inside the moon pool is trapped and thus it moves as a rigid body together with the platform; (2) the moon pool is completely open to the sea and the presence of the water inside the moon pool will not significantly affect the heave motions of the platform. The water in the moon pool has two kinds of natural vibration modes, which are piston-like motion in vertical direction and sloshing motion caused by the free surface (Faltinsen and Timokha, 2009). If the top tension risers are used, the mass of the water inside moon pool is comparable to the mass of the platform. The effect of the motions of water inside the moon pool on the motions of the Spar platform should not be ignored.

Aalbers (1984) assumed that the water column inside a floating vessel can be replaced by a frictionless piston, then the motion equation of water inside the moon pool was derived and the coupled motions were studied. It was found that the water inside the moon pool can decrease the heave amplitude of the vessel. Barreira et al. (2005) treated the motions of water inside a moon pool as a spring-mass system and studied the coupled motions of a mono-column structure and water inside a moon pool. They found that the heave motions of the platform can be decreased by an

* Corresponding author at: State Key Laboratory of Hydraulic Engineering Simulation and Safety Tianjin University, Tianjin 300072, China.
Tel.: +86 22 27406074 811.
E-mail addresses: liu_liqin@eyou.com, liqin.liu@strath.ac.uk (L. Liu).

http://dx.doi.org/10.1016/j.oceaneng.2014.09.048
0029-8018/

appropriate design of a guide plate. Sphaier et al. (2007) presented the mono-column dynamic behavior in waves as obtained from model experiments. They measured the mono-column vertical motions and the motions of water in the moon pool for different opening ratios of the guide plate. The effect of guide plate opening ratios on the heave motions of the platform was analyzed. Gupta et al. (2008) derived a 2-DOF coupling dynamic model of a spar heave and the vertical motion of water inside the moon pool. This work highlights the importance of the moon pool hydrodynamic characteristics in predicting the heave motions of a spar platform. Spanos et al. (2011) developed a 6-DOF nonlinear model, including surge, heave, and pitch motions of a spar platform; surge and heave motions of risers, and vertical motions of water inside the moon pool. The results indicated that the heave amplitude of the platform is reduced significantly by the coupled motions of the platform and water inside the moon pool.

The study presented in this paper investigated the heave motions of a truss spar platform considering the dynamic coupling between the platform motions and the motions of water in the moon pool. The effect of the motions of water on the heave motions of the platform was investigated. The platform heave and the moon pool motions were discussed as opening ratios of the bottom guide plate varied. Three detachable guide plates were designed for the model tests, with 0% opening ratio (moon pool totally closed, Case 1), 30% opening ratio (Case 2) and 70% opening ratio (Case 3). The results of the experiments were used to validate the numerical analysis.

2. Dynamical modeling

The vertical motion equations of water inside the moon pool of a spar platform were derived based on the work of Gupta et al. (2008) through the following steps: (1) the conservation laws of mass and momentum of water inside the moon pool were applied to find the pressure acting on the top of the guide plate; (2) an empirical formula to calculate the pressure acting on the bottom of the guide plate was used; (3) Newton's second law was applied to the fluid in the guide plate gap, to let the pressure difference between two sides of the guide plate accelerate the fluid. The heave equations of the spar platform was established by applying the rigid body dynamics equations given by Liu et al. (2014), and the wave forces were calculated based on the potential theory.

The coordinate system and cross section of the platform hull are shown in Fig. 1. In Fig. 1(a), x axis is in the horizontal plane of the still water, z axis is vertically upward and through the gravity center of the platform, $-z_0$ is the hull static draft, z_1 is the moon pool water surface elevation in the moon pool relative to the horizontal plane of the still water. In Fig. 1(b), S_g is the open area at the bottom of the moon pool, S_o is the area of the guide plate and S_p is the sectional area of the hard tank. The moon pool sectional area can be written as $S_{mp}=S_o+S_g$ and the moon pool opening ratio can be written as S_g/S_{mp}.

First, the motion equation of water in the moon pool in vertical direction is derived. Taking the moon pool water as a deformable control volume, the mass conservation equation is

$$\int_{S_g}\rho(\vec{v}_1-\vec{v}_b)\times\vec{n}dA=-\frac{dM_{mp}}{dt} \tag{1}$$

where ρ is the water density, $\vec{v}_1$ is the velocity of water flowing through the guide plate gap, the magnitude is v_g, $\vec{v}_b$ is the velocity of the spar platform heave, the magnitude is $\dot{z}$, $\vec{n}$ is unit outward normal vector, $M_{mp}=\rho S_{mp}(z_1-z-z_0)$ is the mass of the moon pool water. Substituting above parameters into Eq. (1) leads to

$$v_g=\frac{\dot{z}+S_{mp}}{S_g\times(\dot{z}_1-\dot{z})} \tag{2}$$

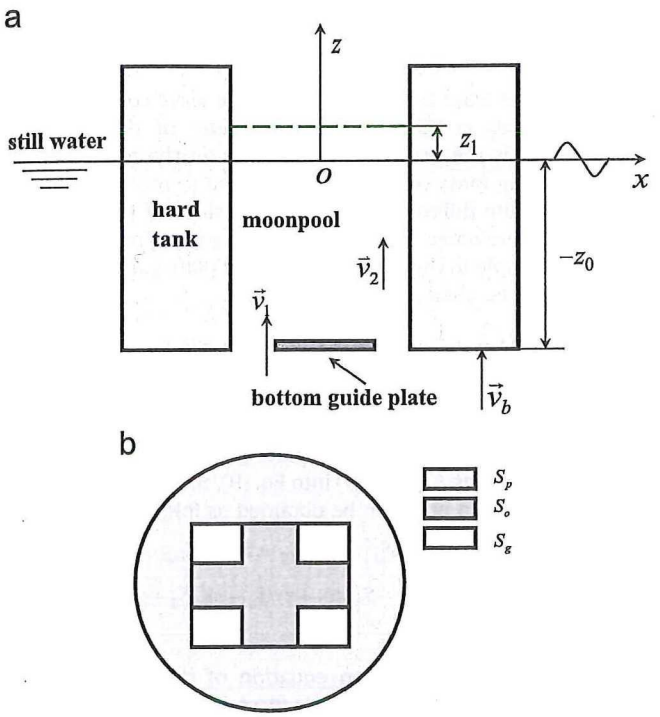

Fig. 1. Coordinate system and cross section of the hull of the platform: (a) coordinate system, (b) cross section.

The linear momentum equation of the deformable control volume can be written as Hansen (1967)

$$\sum\vec{F}=\frac{d}{dt}\left(\int_{CV}\vec{V}\rho d\forall\right)+\int_{CS}\vec{V}\rho(\vec{V}_r\times\vec{n})dA \tag{3}$$

where $\vec{V}$ is fluid velocity vector in the control volume CV, $\vec{V}_r$ is the fluid velocity vector cross the control surface CS.

To simplify the analysis, assuming the flow properties over the cross section and those inside the control volume are uniform, respectively (White, 2003), the right hand side of Eq. (3) can be further written as

$$\frac{d}{dt}\left(\int_{CV}\rho\vec{v}_2 d\forall\right)+\int_{S_g}\rho\vec{v}_2(\vec{v}_1-\vec{v}_b)\times\vec{n}dA=\frac{d}{dt}\{\rho\dot{z}_1S_{mp}(z_1-z-z_0)\}-\rho\dot{z}_1(v_g-\dot{z})S_g \tag{4}$$

where $\vec{v}_2$ is the velocity of the water particle inside the moon pool, the magnitude is $\dot{z}_1$.

The left hand side of Eq. (3) includes surface force acting on the control surface and mass force acting on the water particles inside the moon pool. The forces can be written as

$$\sum\vec{F}=-\rho gS_{mp}(z_1-z-z_0)+p_1S_{mp} \tag{5}$$

where p_1 is the pressure on the upper side of the guide plate, g is the acceleration of gravity.

Substituting Eqs. (4) and (5) into Eq. (3) yields the relation

$$\rho\ddot{z}_1S_{mp}(z_1-z-z_0)=-\rho gS_{mp}(z_1-z-z_0)+p_1S_{mp} \tag{6}$$

From Eq. (6), p_1 can be derived as

$$p_1=\rho(\ddot{z}_1+g)(z_1-z-z_0) \tag{7}$$

The pressure on the lower side of the guide plate includes the static pressure, the inertia force due to vertical acceleration, the dynamic pressure due to velocity and the incident wave pressure.

It can be given by a semi-empirical formula (Gupta et al., 2008)

$$p_2 = -\rho g(z+z_0) - \alpha_3 \rho d_g \ddot{z} + \gamma \rho d_g a_w + p_w \tag{8}$$

where γ is the wave acceleration, α_w is the wave coefficient in the moon pool, d_g is the equivalent diameter of the moon pool opening, p_w is the wave pressure acting on the guide plate, α_3 is the coupling mass coefficient of platform to moon pool.

The pressure difference between two sides of the guide plate accelerates the water in the guide plate gap. Applying the force balance principle to the water in the guide plate gap, the following equation can be obtained

$$(p_2 - p_1)S_g = M_g \dot{v}_g + \frac{1}{2}\rho(v_w - v_g + \dot{z})|v_w - v_g + \dot{z}|K_g S_g \tag{9}$$

where $M_g = \rho \alpha_1 S_g d_g$, α_1 is the added mass coefficient of the moon pool, v_w is the wave velocity, K_g is the damping coefficient of the water flowing through the guide plate gap.

Substituting Eqs. (7) and (8) into Eq. (9), the motion equation of water in the moon pool can be obtained as follows

$$\begin{aligned}&\ddot{z}_1[\rho\alpha_1 d_g S_{mp} + (z_1 - z - z_0)\rho S_g] + z_1 \rho g S_g = \ddot{z}[\rho\alpha_1(S_{mp} - S_g)d_g - \rho\alpha_3 d_g S_g] \\ &+ [v_w - S_{mp}(\dot{z}_1 - \dot{z})/S_g]|v_w - S_{mp}(\dot{z}_1 - \dot{z})/S_g|\frac{1}{2}\rho K_g S_g + p_w S_g + \gamma\rho\alpha_w d_g S_g\end{aligned} \tag{10}$$

Second, the heave motion equation of the spar platform is established. Considering the inertia force, restoring force, damping force, wave force and force from the moon pool water, the heave motion equation of the spar platform can be written as

$$\ddot{z}(M + \Delta M) + \rho g S_m z + B_1 \dot{z} + B_2 \dot{z}|\dot{z}| = p_w S_p + F_m \tag{11}$$

where M is the platform mass, ΔM is the heave added mass, S_m is the water plane area of the platform hull, B_1 is the linear damping coefficient, B_2 is the quadratic damping coefficient, F_m is the force acting on the guide plate. The risers and the mooring system are not considered here.

Weggel and Roesset (1994) derived the expression of total vertical diffraction force acting on truncated cylinder. Based on their work, the wave pressure acting on the Spar platform in heave direction can be represented as

$$p_w = \rho g H_w \left[1 - \frac{1}{2}\sin(kR)\right]\left(\frac{J_1(kR)}{kR}\right)e^{kz_0}\cos(\omega t - \varepsilon) \tag{12}$$

where H_w is the wave height, R is the hull radius, k is the wave number, J_1 is the first kind Bessel function, ω is the wave frequency, $\varepsilon = 31\pi(kR)^{1.3}/180$.

The force acting on the guide plate can be divided into two parts as

$$F_m = F_p + F_c \tag{13}$$

The first term in the right hand side of Eq. (13) is the pressure force, it can be represented as

$$F_p = (p_2 - p_1)(S_{mp} - S_g) \tag{14}$$

To simplify the calculation, only the static parts of p_2 are considered. Substituting Eqs. (7) and (8) into Eq. (14) leads to

$$F_p = \{p_w - z_1\rho g - \ddot{z}_1(z_1 - z)\rho + \ddot{z}_1\rho z_0\}(S_{mp} - S_g) \tag{15}$$

The second term on the right hand side of Eq. (13) is a correction term, it accounts for the effect of the net fluid acceleration on the pressure acting on the platform's bottom. It can be represented by a semi-empirical formula (Gupta et al., 2008), as follows

$$F_c = (\ddot{z} - \ddot{z}_1)\rho\alpha_4 d_g(S_p + S_{mp} - S_g) \tag{16}$$

where α_4 is the coupling mass coefficient of moon pool to platform.

Substituting Eqs. (13), (15) and (16) into Eq. (11), the heave motion equation of the platform can be expressed as

$$\begin{aligned}&\ddot{z}[M + \Delta M - \rho\alpha_4 d_g(S_p + S_{mp} - S_g)] + z\rho g S_m + B_1\dot{z} + B_2\dot{z}|\dot{z}| = p_w(S_p + S_{mp} - S_g) \\ &- z_1\rho g(S_{mp} - S_g) - \ddot{z}_1(z_1 - z)\rho(S_{mp} - S_g) + \ddot{z}_1[\rho(S_{mp} - S_g)z_0 - \rho\alpha_4 d_g(S_p + S_{mp} - S_g)]\end{aligned} \tag{17}$$

Eqs. (10) and (17) can be combined to form the 2-DOF coupling motion equations of the heave motions of the Spar platform and the vertical motions of the moon pool water. The coupling terms include the inertia force, the damping force, the restoring force and the added mass came from the mass coupling between the platform and the moon pool.

3. Platform parameters

A hypothetical spar platform geometry was used to carry out the analysis, which is similar to Horn Mountain platform (Petter, 2000). The platform parameters are shown in Table 1.

The risers of Horn Mountain Spar platform are supported by a buoyancy tanks. For the present hypothetical platform, the top tension risers are used. The objective is to investigate the effect of water motions in the moon pool on the heave motions of the spar platform. Three cases are considered as listed in Table 1, including the moon pool is totally closed (Case 1), 30% of the moon pool is open (Case 2) and 70% of the moon pool is open (Case 3). The draft and the CG (center of gravity) of the platform are equal for the three cases. The natural heave period of the platform for Case 1 is $t_s = 24.4$ s, for Case 2 and Case 3 is $t_s = 26.8$ s. Using the empirical relation $t_m = 2\pi\sqrt{d/g}$, where d is the draft of hull, the natural period of the moon pool motions in the vertical direction is $t_m = 14.7$ s.

4. Numerical simulation results and discussion

The heave responses of the platform and vertical motions of water in the moon pool are predicted in this section. For the truss spar platform, the radiation damping is insignificant relative to the viscous damping (Lu et al., 2003; Ghosh and Spanos, 2009), therefore it is neglected and only the nonlinear damping is considered in the following calculations. The nonlinear damping coefficients for the three cases are obtained from the model experiments as detailed in Section 6. The initial values of the coupling parameters and the moon pool hydrodynamic coefficients are $\alpha_1 = 0.326$, $\alpha_3 = \alpha_4 = 0.5$, $\alpha_w = 1.45$ and $K_g = 1.0$. Their effects on the responses will be analyzed in Section 5.

Solving Eqs. (10) and (17) by Runge–Kutta method, the time histories of the platform heave responses z and the vertical

Table 1
Platform parameters.

Description	Value
Water depth	1652 m
Total length	169.16 m
Diameter of hard tank	32.31 m
Draft	153.92 m
Center of gravity from keel	90.39 m
Moon pool	15.85 × 15.85 m^2
Length of hard tank	68.88 m
Number of heave plates	3
Opening ratio/Case 1	0% (Moon pool totally closed)
Opening ratio/Case 2	30%
Opening ratio/Case 3	70%

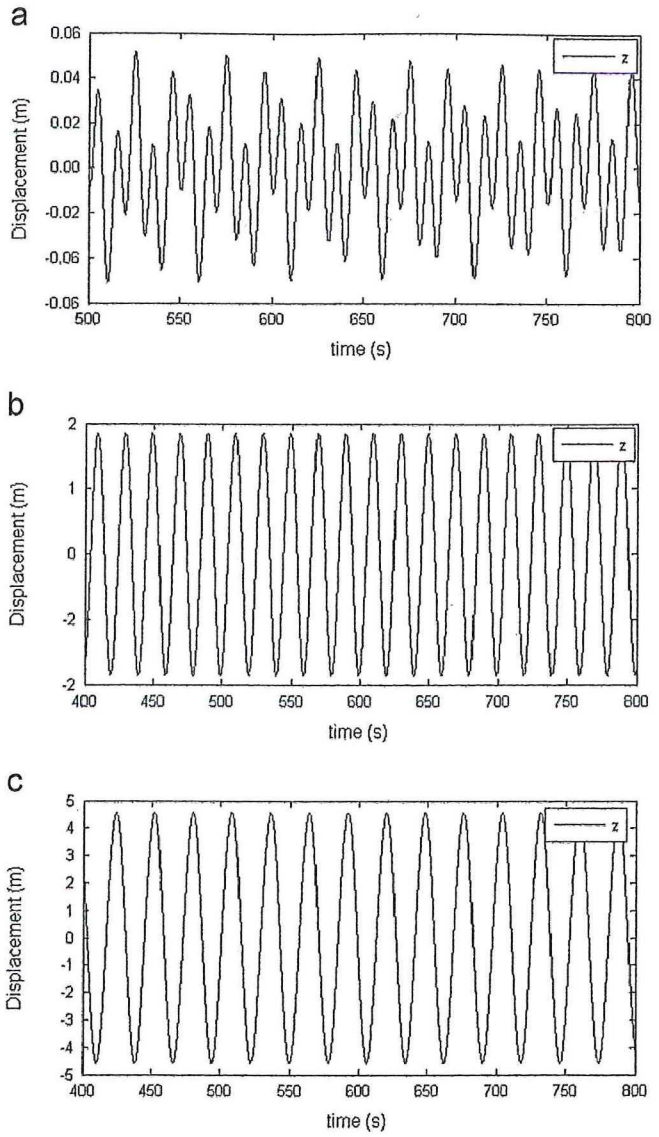

Fig. 2. Response time histories for Case 1, wave height 4 m: (a) wave period 10 s, (b) wave period 20 s, (c) wave period 28 s.

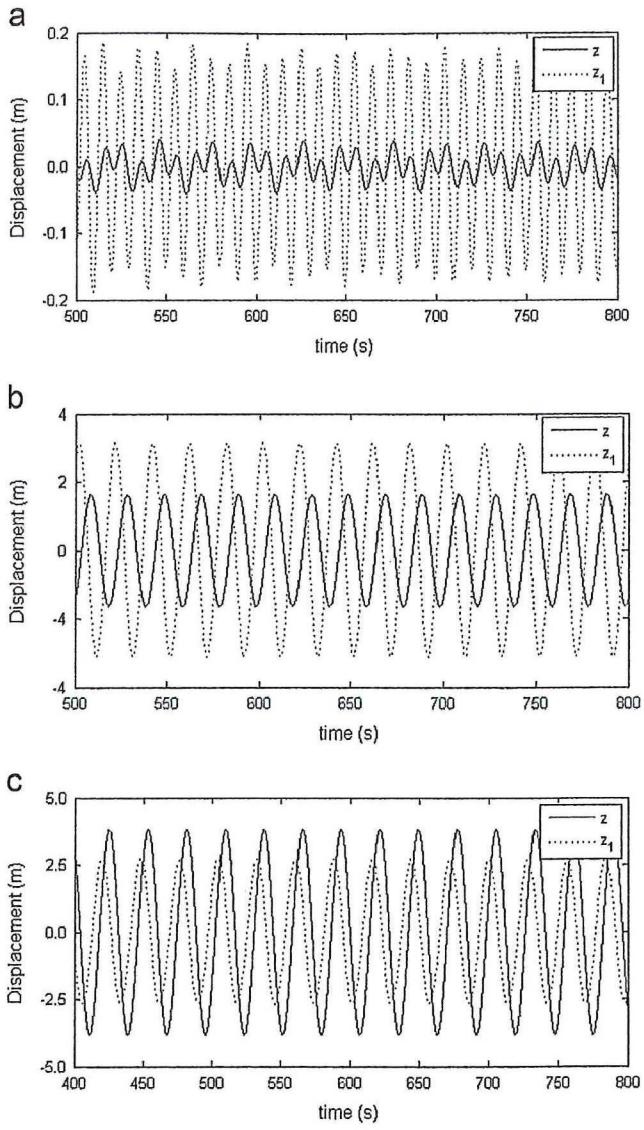

Fig. 3. Response time histories for Case 2, wave height 4 m: (a) wave period 10 s, (b) wave period 20 s, (c) wave period 28 s.

motions of water in the moon z_1 are obtained, as shown in Figs. 2–4.

It is observed that for Case 2 and Case 3, the amplitudes of z and z_1 depend on the wave period. When the wave period is close to t_m (the natural period of water motions in vertical direction in the moon pool), larger vertical motions of the moon pool are excited. When the wave period is close to t_s (the natural period of the platform heave), larger heave motions of the platform are excited. For the shorter wave periods, the platform heave and the moon pool motions are nonlinear, as shown in Fig. 2(a) and Fig. 4(a).

In order to consider the nonlinear damping sufficiently, amplitude response curves of the platform heave and the moon pool motions are calculated using a numerical iterative method (Li and Ou, 2009) through the following steps: (1) the mean response amplitudes of the platform heave and the moon pool motions are calculated when $h_w = 4\ m$ as wave periods vary; (2) each response amplitude is divided by the wave amplitude. The results for above three cases are shown in Fig. 5.

In Fig. 5, m_a and p_a indicate amplitudes of the moon pool motions and the heave motions of the platform, respectively, w_a indicates the wave amplitude. It is observed that the motions of the moon pool greatly depend on the opening ratio of the moon pool. Comparing with Case 2, the maximum amplitude of the moon pool motions in Case 3 is nearly 2.4 times of those in Case 2 and large amplitude motions of the moon pool are excited. The maximum heave amplitudes of the platform in Case 2 and Case 3 are smaller than those of Case 1, and the platform heave motions decrease for the semi-closed cases comparing with the totally closed case. The maximum values of p_a/w_a in Case 1, Case 2 and Case 3 are 2.33, 1.92 and 2.08, respectively, as shown in Fig. 5(b). Comparing with Case 1, it reduces nearly 17.6% in Case 2 and reduces nearly 10.7% in Case 3.

For Case 3, heave response amplitude curve of the platform has two peaks, one is close to t_s and the other one is close to t_m. When the wave period is close to t_m, large heave motions of the platform are excited due to large amplitude motion of the moon pool and the energy is transferred to the platform due to the dynamic coupling.

5. Parametric analysis

In this section, the amplitude response curves as stated in Section 4 are calculated for the cases of 30% and 70% opening ratios to investigate the effects of coupling parameters.

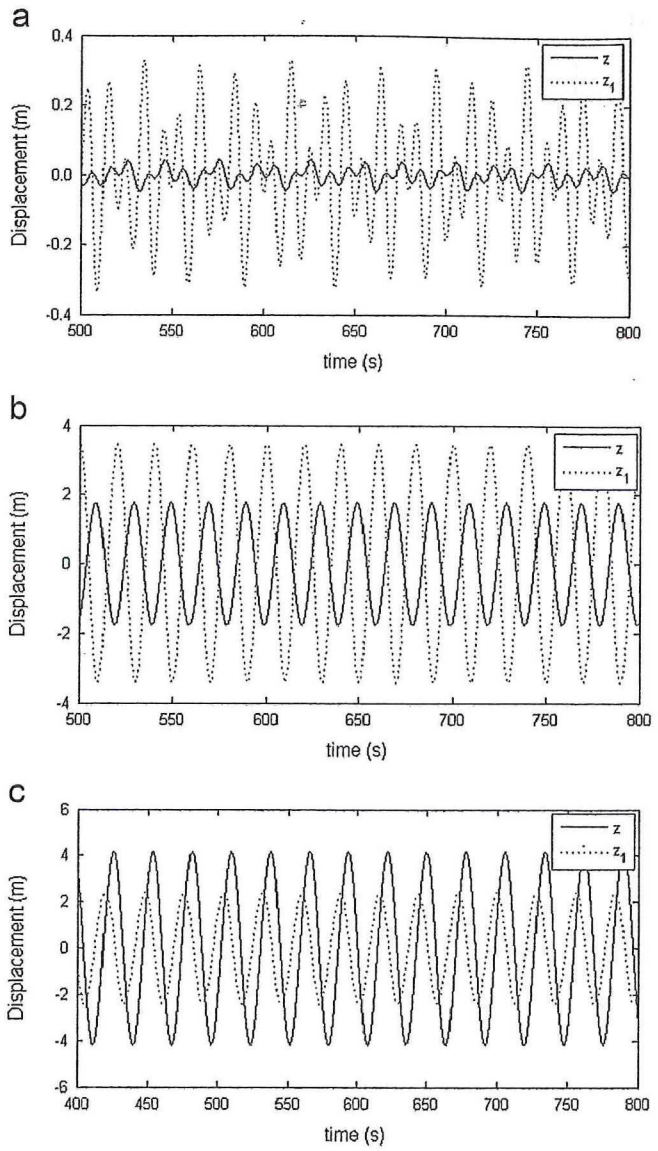

Fig. 4. Response time histories for Case 3, wave height 4 m: (a) wave period 10 s, (b) wave period 20 s, (c) wave period 28 s.

5.1. Coupling mass coefficients

The influences of the coupling mass coefficients α_3 and α_4 are investigated by calculating the response amplitude curves for the different coefficient values, as shown in Figs. 6–9.

It can be seen that α_3 greatly affects the vertical motions of the water inside the moon pool, the amplitude and the natural period of the moon pool motions increase with the increase of α_3, since α_3 affects the inertia force of moon pool motions. In Case 3, when the wave period is close to t_m, α_3 obviously affects the platform heave motions because of strong dynamic coupling between the moon pool and the platform heave, as shown in Fig. 7(a). α_4 affects the platform heave and it increases with the increase of α_4. Especially in Case 3, the smaller peak of the heave response amplitude curve of the platform becomes more obvious with the increase of α_4, as shown in Fig. 9(a).

5.2. Hydrodynamic coefficients of water in the moon pool

This section discusses the influences of hydrodynamic coefficients of the water in the moon pool, including α_1, K_g and α_w, the results are shown in Figs. 10–15.

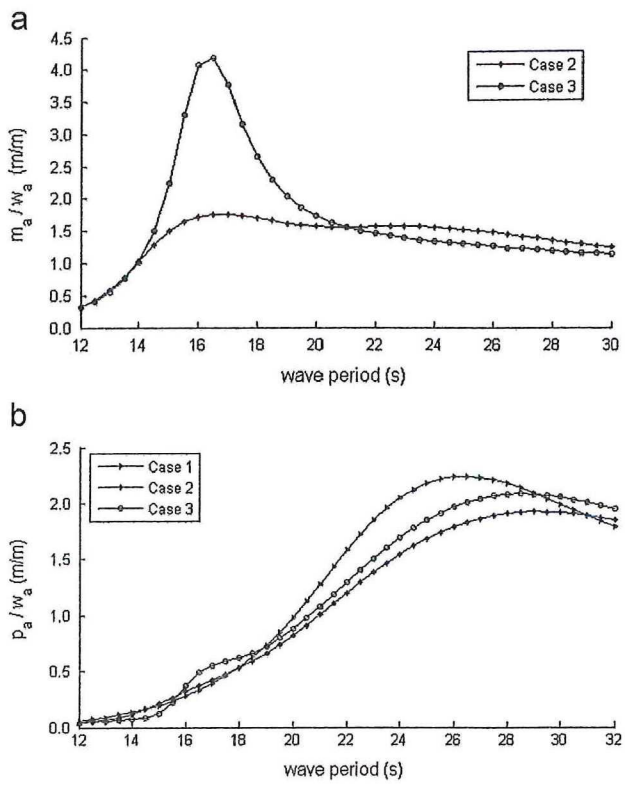

Fig. 5. Response amplitude operator curves: (a) the moon pool motions, (b) the platform motions.

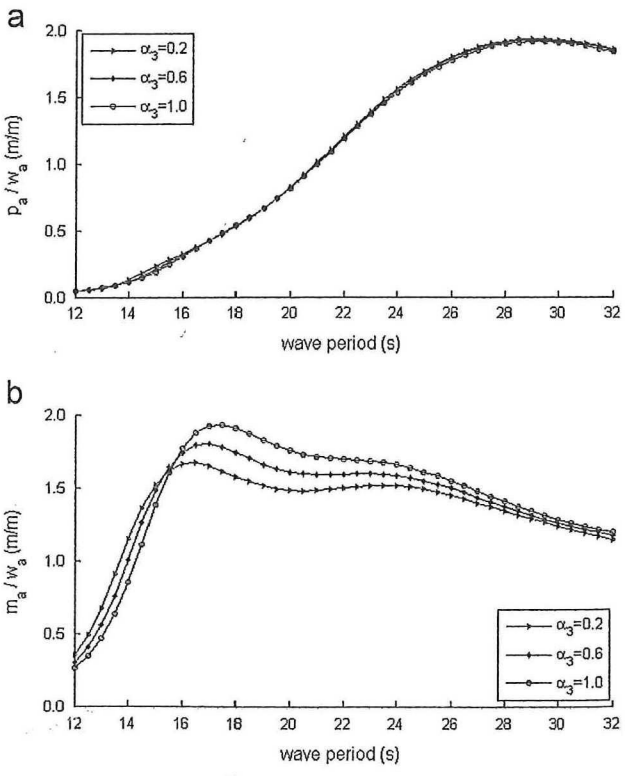

Fig. 6. Effect of α_3 on platform and moon pool motions, Case 2: (a) platform heave motions, (b) vertical moon pool motions.

It can be found that α_1 affects the inertia force of moon pool motions and therefore greatly affects the amplitude and the natural period of the moon pool motions, as shown in Fig. 10(b)

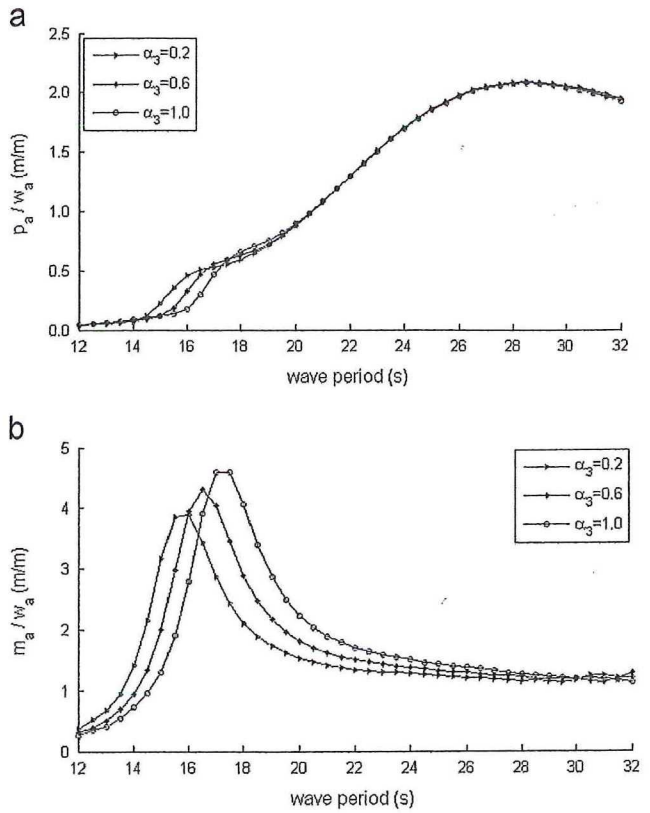

Fig. 7. Effect of α_3 on platform and moon pool motions, Case 3: (a) platform heave motions, (b) vertical moon pool motions.

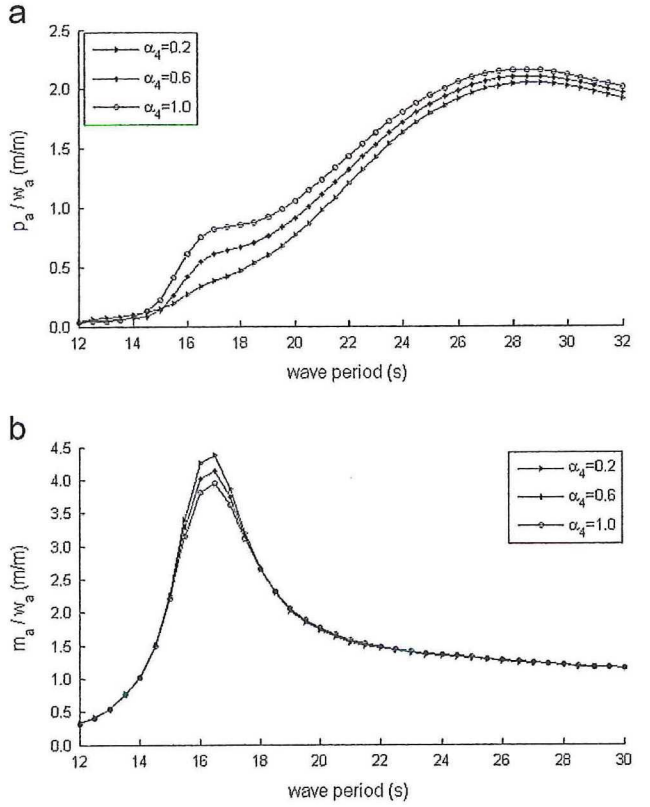

Fig. 9. Effect of α_4 on platform and moon pool motions, Case 3: (a) platform heave motions, (b) vertical moon pool motions.

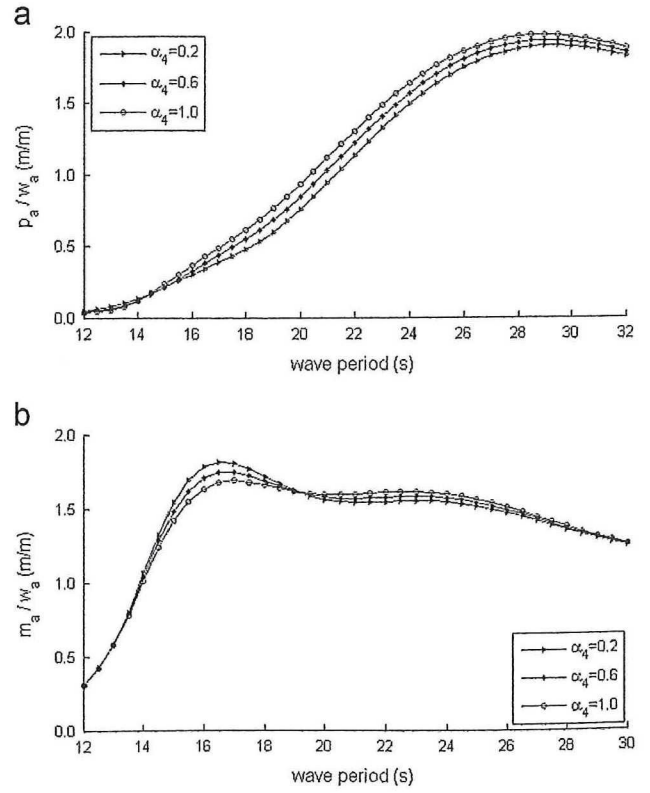

Fig. 8. Effect of α_4 on platform and moon pool motions, Case 2: (a) platform heave motions, (b) vertical moon pool motions.

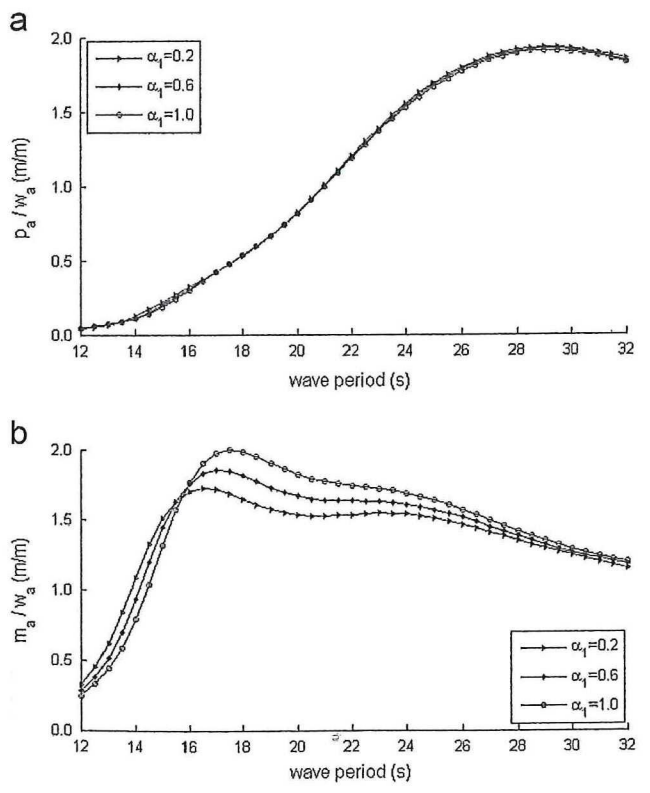

Fig. 10. Effect of α_1 on platform and moon pool motions, Case 2: (a) platform heave motions, (b) vertical moon pool motions.

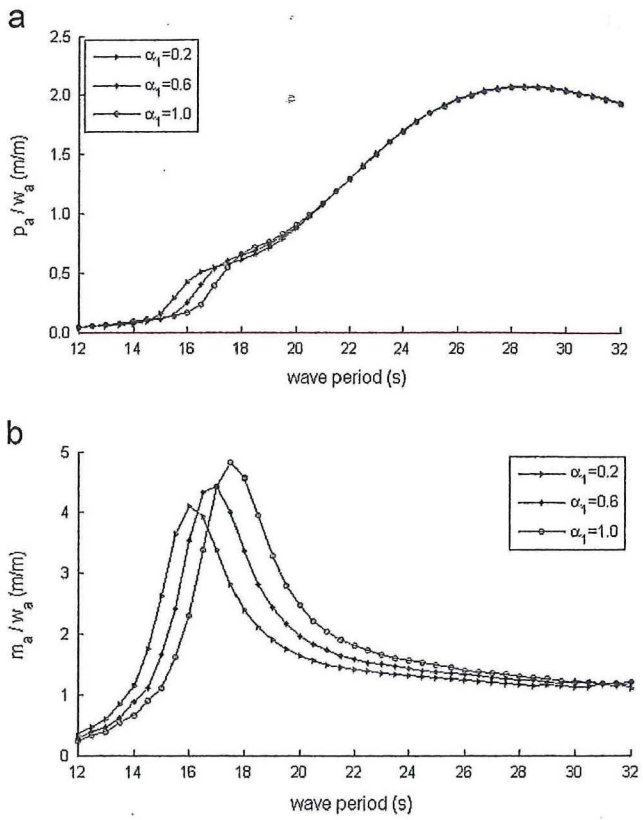

Fig. 11. Effect of α_1 on platform and moon pool motions, Case 3: (a) platform heave motions, (b) vertical moon pool motions.

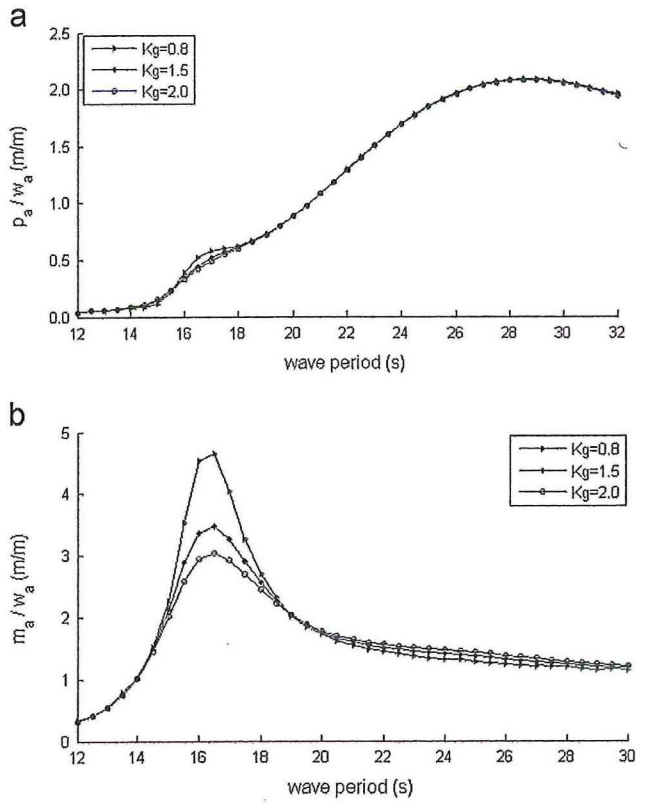

Fig. 13. Effect of K_g on platform and moon pool motions, Case 3: (a) platform heave motions, (b) vertical moon pool motions.

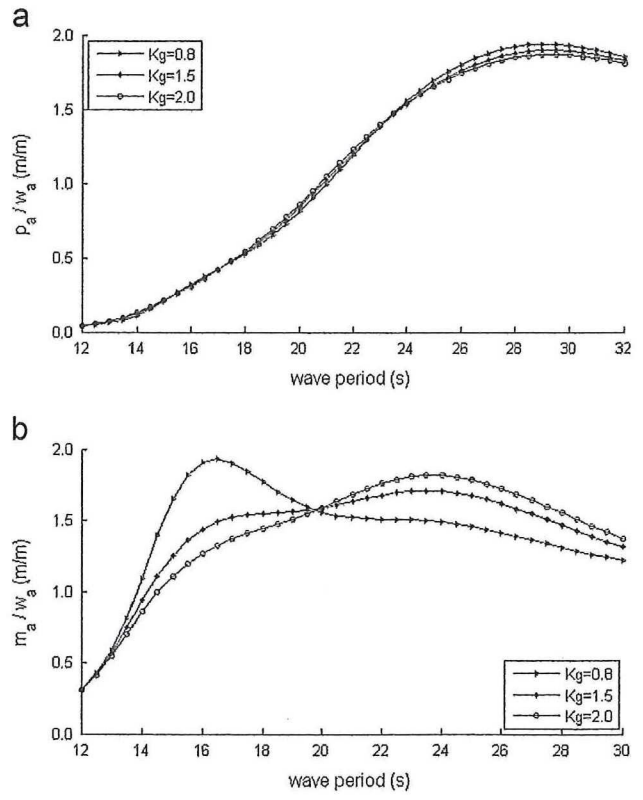

Fig. 12. Effect of K_g on platform and moon pool motions, Case 2: (a) platform heave motions, (b) vertical moon pool motions.

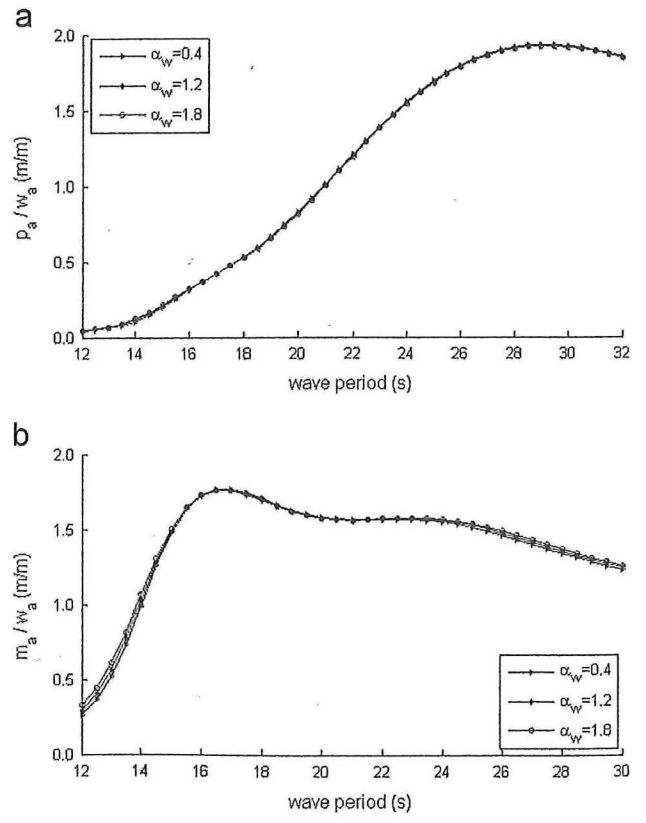

Fig. 14. Effect of α_w on platform and moon pool motions, Case 2: (a) platform heave motions, (b) vertical moon pool motions.

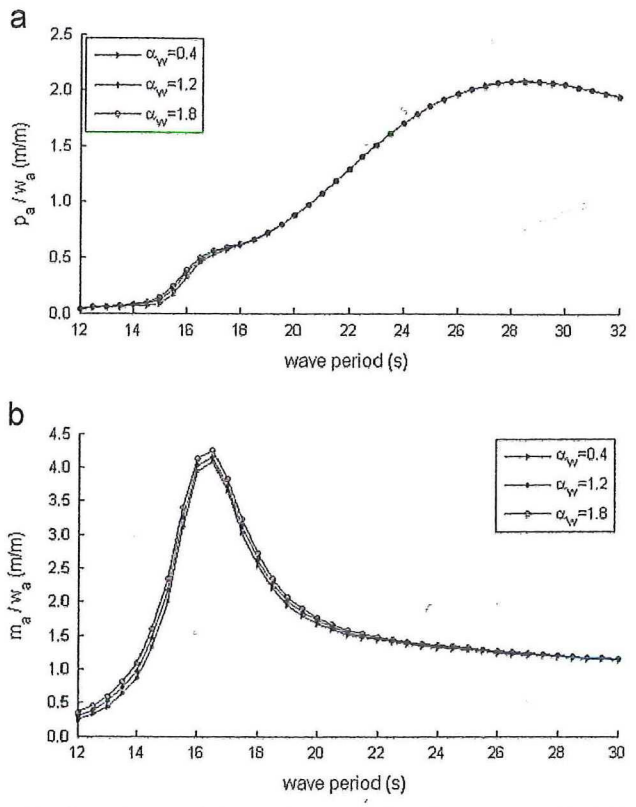

Fig. 15. Effect of α_w on platform and moon pool motions, Case 3: (a) platform heave motions, (b) vertical moon pool motions.

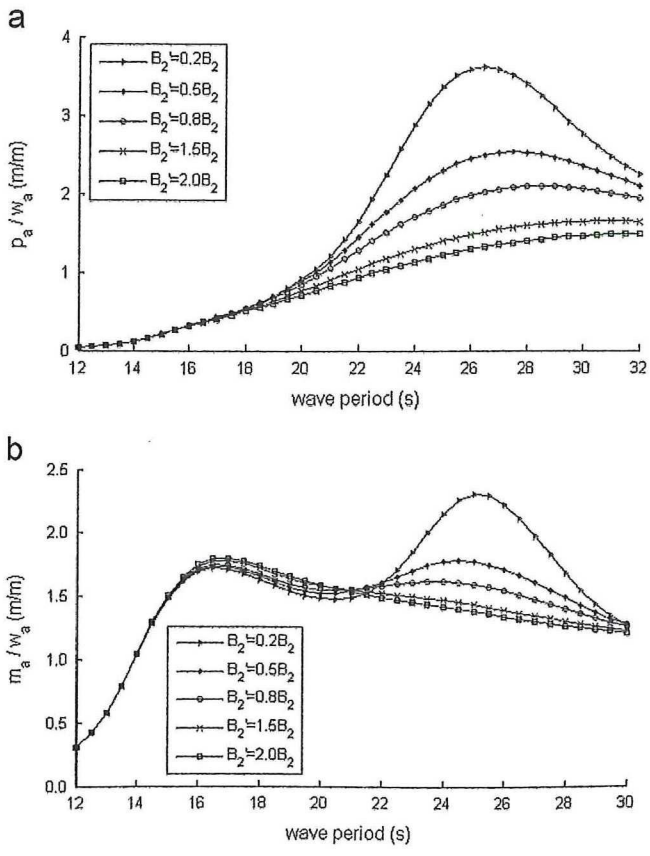

Fig. 16. Effect of nonlinear damping coefficients, Case 2: (a) platform heave motions, (b) vertical moon pool motions.

and Fig. 11(b). The motions of the moon pool are sensitive to K_g and it decreases with the increase of K_g, for example, in Fig. 13(b) when K_g increases from 0.8 to 1.5, the maximum value of m_a/w_a decreases nearly 25%.

For Case 3, α_1 and K_g affect amplitude of the heave motions of the platform when wave period is close to t_m, as Fig. 11(a) and Fig. 13(a) showing. The reason is that the motions of the moon pool are greatly affected by α_1 and K_g, the energy is transferred to the platform heave due to strong dynamic coupling when the opening ratio is large. Coefficient α_w has little effect on the platform heave and the moon pool motions, as shown in Figs. 14 and 15.

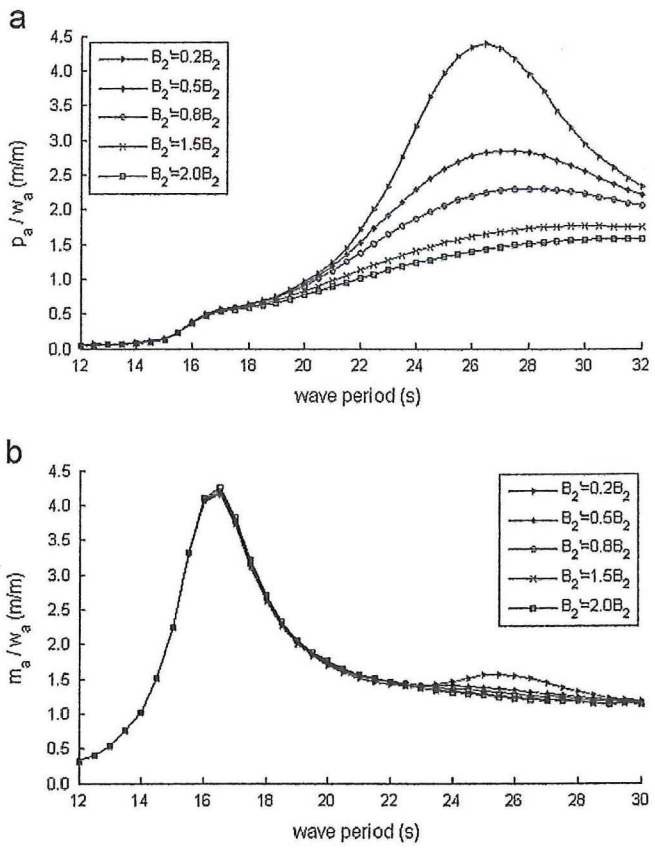

Fig. 17. Effect of nonlinear damping coefficients, Case 3: (a) platform heave motions, (b) vertical moon pool motions.

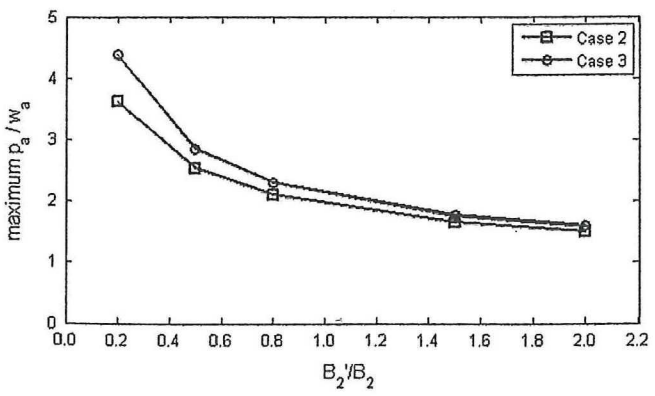

Fig. 18. Maximum values of heave response amplitude curves of the platform.

5.3. Damping coefficients

This section discusses the influence of damping coefficients. The initial damping coefficient B_2 is obtained from model experiments, as presented in Table 3 of Section 6. The response amplitude curves for different nonlinear damping coefficients $0.2B_2$, $0.5B_2$, $0.8B_2$, $1.5B_2$ and $2.0B_2$ are calculated and the results are shown in Figs. 16 and 17. The maximum values of heave response amplitude curves of the platform for different damping coefficients are shown in Fig. 18.

Fig. 16(a) and Fig. 17(a) show that the heave motions of the platform decreases with the increase of nonlinear damping. The response amplitude curve of the moon pool motions has two peaks for lower nonlinear damping, one is near to the natural period of the moon pool the other is near to the natural heave period of the platform, as shown in Fig. 16(b) and Fig. 17(b). This indicates that the effect of the platform heave on the moon pool water motions becomes important for the lower nonlinear damping, especially in the case of smaller moon pool opening ratio.

It is observed from Fig. 18 that the maximum values of the heave response amplitude curves of the platform nonlinearly decrease with the increase of nonlinear damping. When the nonlinear damping coefficient increases from $0.2B_2$ to $0.5B_2$ the platform heave decreases sharply. Comparing Case 2 with Case 3, the heave motions of the platform are greatly affected by the nonlinear damping in Case 3.

6. Model experiments

The model experiments were used to study the effect of the moon pool water on the heave motions of the truss Spar platform. The experiments were carried out in Tianjin University's wave tank with size of 137 m long, 7 m wide, and 3.5 m deep and is equipped with a flap type wave maker. The wave lengths made by the wave maker are from 2 m to 12 m.

6.1. The model and test conditions

The model scale 1:130 was selected taking into consideration the size of the tank and the wave making capacity of the wave maker. Model parameters are shown in Table 2.

Three detachable bottom guide plates with different opening ratios were constructed and three test cases were carried out including 0% opening ratio (moon pool was totally closed, Case1), 30% opening ratio (Case 2) and 70% opening ratio (Case 3) as illustrated in Fig. 19, which shows the photographs of guide plates installed on the platform (photographed from top to bottom of the moon pool). Drafts of the platform were kept constant and the centre of gravities were almost equal for the three cases.

The motions of the model were measured in regular waves. The heave natural periods of the platform for three cases are from 24 s to 27 s and the natural period of vertical motion of water inside the moon pool is 14.7 s. So, in the experiment the wave periods were changed from 12 s to 32 s and the wave height 4 m was selected.

Table 2
Model parameters.

Parameter	Unit	Value
Total length	m	1.300
Draft	m	1.185
Total displacement	t	0.021
Diameter of hard tank	m	0.249
Length of hard tank	m	0.530
Heave plates space	m	0.176
Cross section area of heave plate	m^2	0.249×0.249
Cross section area of moon pool	m^2	0.120×0.120

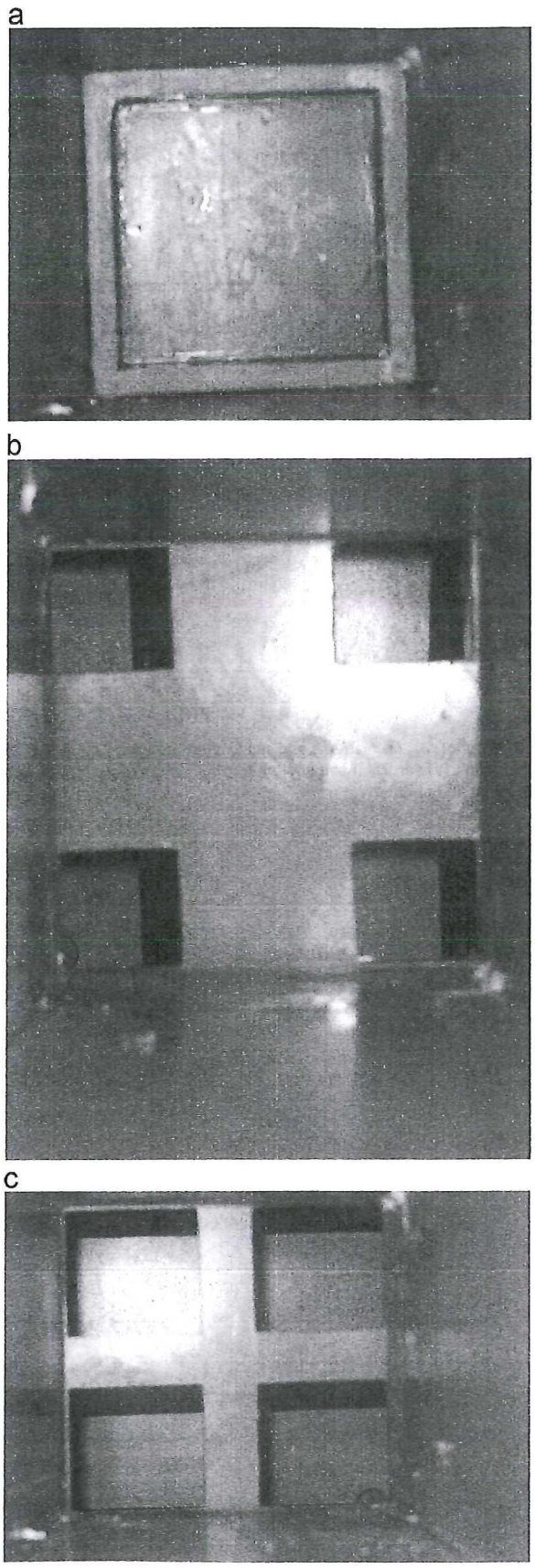

Fig. 19. Three different bottom guide plates: (a) Case 1, (b) Case 2, (c) Case 3.

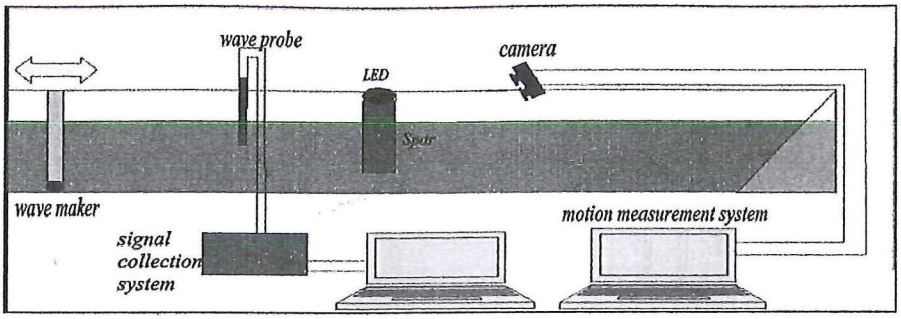

Fig. 20. Sketch of the test setup.

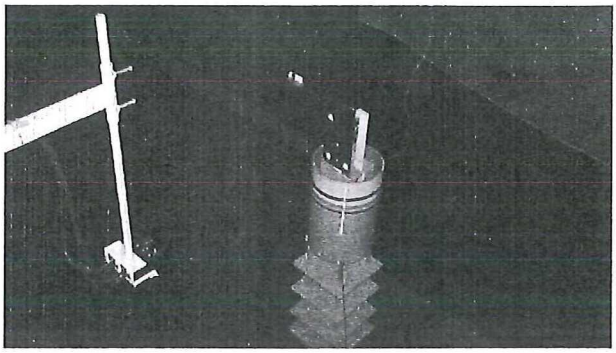

Fig. 21. The test layout.

6.2. The test setup

A wave probe and an optical motions measurement system were used to measure the incident wave displacement and 6-DOF motions of the model as illustrated in Fig. 20, which shows the sketch of test setup. The model was moored by four springs attached at the center of pitch to limit the horizontal motions, three LEDs were mounted on the top of the model to mark the motions of the model as illustrated in Fig. 21. The camera was mounted in a steel frame fixed in towing tank. The distance between the camera to the model is about 1.5 m.

Before the test, the wave probe and the optical motion measuring instrument were calibrated. For all the tests, the camera was kept fixed in order to minimize the errors in measured results. Each test can't be carried out until the water surface becomes calm. Data were collected before the front of the first wave reaches the wave probe and were stopped as soon as the wave reaches the beach at the far end of the towing tank. Only the harmonic part of the measured signal were used in the following motions analyses. The measured results can be applied to validate the numerical solution. In following Sections 6.3 and 6.4 all the data presented were in the prototype scale.

6.3. Spar platform motions in calm water

The heave free decay motions of the spar platform in calm water were measured for the three cases and the damping coefficients were obtained.

The motion equation can be written as

$$\ddot{x}+d_1\dot{x}+d_2\dot{x}|\dot{x}|+d_3x=0 \tag{18}$$

where d_1 is the linear damping coefficient and d_2 is the quadratic damping coefficient. d_1 and d_2 can be determined by the free decay motions using the method proposed by Faltinsen (1990). Only the nonlinear damping coefficient d_2 was considered here.

Table 3
Natural period of the platform heave and nonlinear damping coefficient.

	Heave natural period (s)	Damping coefficient d_2
Case 1	24.40	0.0797
Case 2	26.79	0.1211
Case 3	26.79	0.1126

The heave natural period was obtained by average of 10 consecutive period cycles of the free decay test. The results for the three cases are shown in Table 3.

Table 3 shows that natural period of the spar platform in heave in Case 2 and Case 3 are longer than that in Case 1. Comparing with Case 1, d_2 increases about 52% in Case 2 and increases about 41% in Case 3. The nonlinear damping of the platform in heave is much more enhanced for the cases of semi-closed moon pool. Comparing Case 2 with Case 3, d_2 decreases a little in Case 3.

6.4. Spar platform motion in waves

The 6-DOF motions of the Spar platform were tested in different waves and the platform heave motions were analyzed. Some response curves of the platform heave are shown in Figs. 22–24, the amplitude response curves for the three cases are shown in Fig. 25.

It can be found that the heave amplitude of the platform increases with the wave period approaching natural period of the platform in heave, and the heave responses are nonlinear for the shorter wave periods, as shown in Fig. 22(a), Fig. 23(a) and Fig. 24(a). These conclusions agree with the numerical results of Figs. 2–4.

To make a comparison between the results of numerical calculation and those of model test, the results of numerical calculation were also presented in Fig. 25(a). It is shown that the maximum heave amplitude of the platform in Case 1 is bigger than those in Case 2 and Case 3. Comparing with Case 1, it decreases nearly 20% in Case 2 and decreases nearly 13% in Case 3. This agrees well with the numerical results and approves validity of the dynamic predictions.

There are two peaks in the heave response amplitude curve of the platform for Case 3, the higher one is near to the heave natural period of the platform and the lower one is near natural period of motions of the water inside the moon pool as shown in Fig. 25(b). The results agree with the numerical results of Section 4. The maximum value of the lower peak of the tests is smaller than that of the numerical calculations. Since it is difficult to exactly match the wave period generated by the wave maker to the natural period of water motions in vertical direction inside the moon pool in the model experiment. The dynamical equations only considered the heave motions of the platform, while in the test the

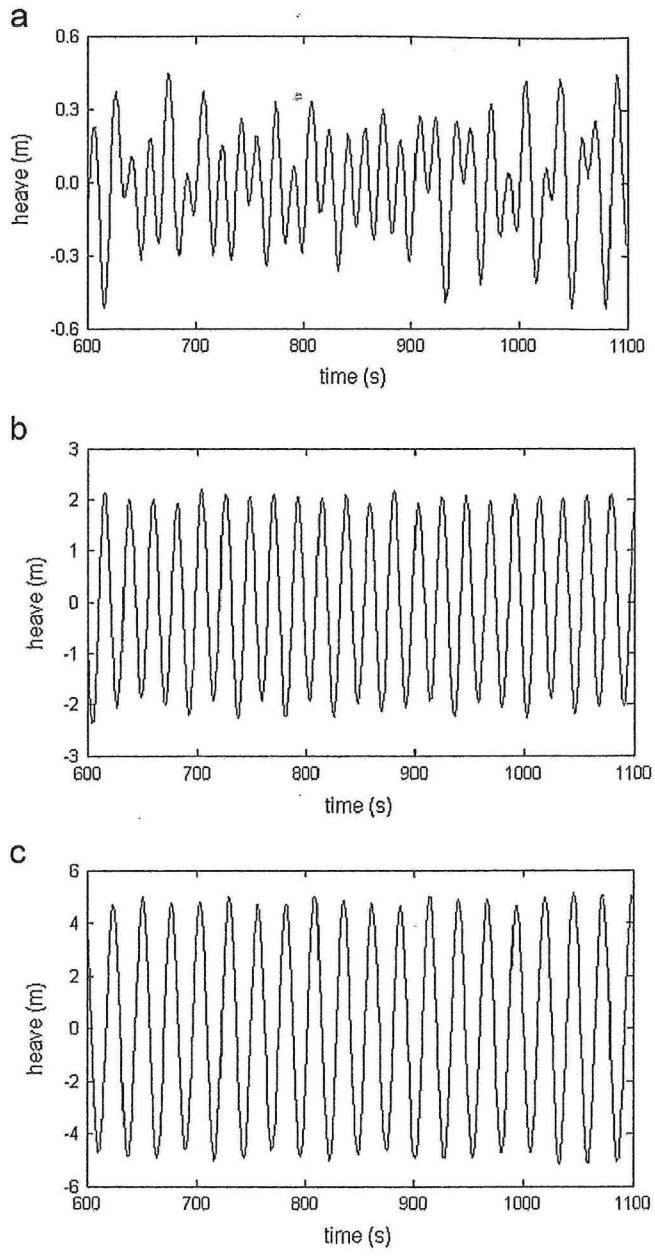

Fig. 22. Platform heave time histories for Case 1, wave height 4 m: (a) wave period 16.5 s, (b) wave period 22.0 s, (c) wave period 26.2 s.

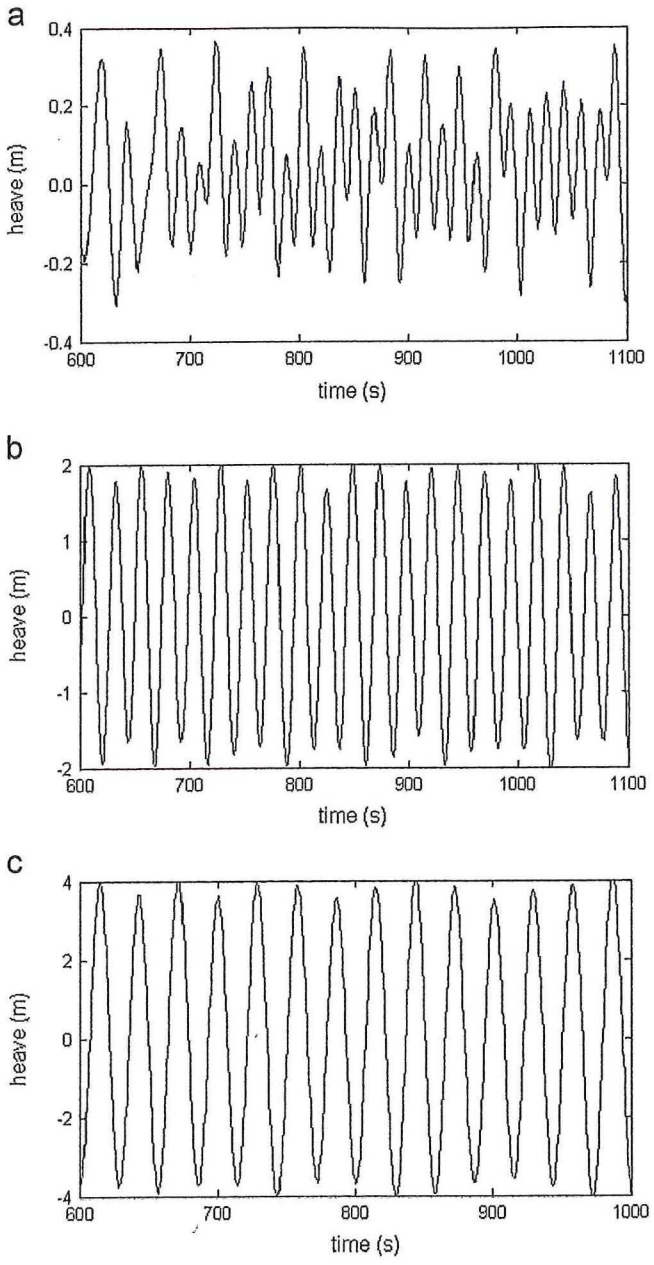

Fig. 23. Platform heave time histories for Case 2, wave height 4 m: (a) wave period 15.8 s, (b) wave period 23.9 s, (c) wave period 28.5 s.

model has 6-DOF motions. This leads to the difference between the RAO curves obtained by the model test and those obtained by the numerical calculation.

7. Conclusions

The research reported in this paper investigated the heave response of a truss Spar platform with semi-closed moon pool. The 2-DOF coupled dynamic motion equations of the platform in heave and the vertical water motions in the moon pool were derived. The calculations and experimental measurements were carried out for three cases where the moon pool was totally closed, 30% and 70% open. The effect of the moon pool motions on the heave motions of the platform was analyzed. The heave characteristics of the platform and the vertical motions of the moon pool were discussed for different parameters. Model experiments were carried out to validate the numerical calculations. The main conclusions are listed as follows:

(1) Comparing the case when the moon pool was totally closed with the cases when the moon pool was partially closed, the heave motions of the platform decrease in the cases of semi-closed moon pool. Different moon pool opening ratios result in different amplitudes of the heave motions of the platform. In the actual design, an optimized opening ratio can be determined to decrease heave of the spar platform. In the present study the heave motions of the platform are lower in case of 30% opening ratio.
(2) A lower peak appears in the heave response amplitude curves of the platform in Case 3 when wave period is near to the natural period of the moon pool motions (t_m). The reason is that when the wave period is close to t_m, larger moon pool motion amplitudes are excited and energy is transferred to the

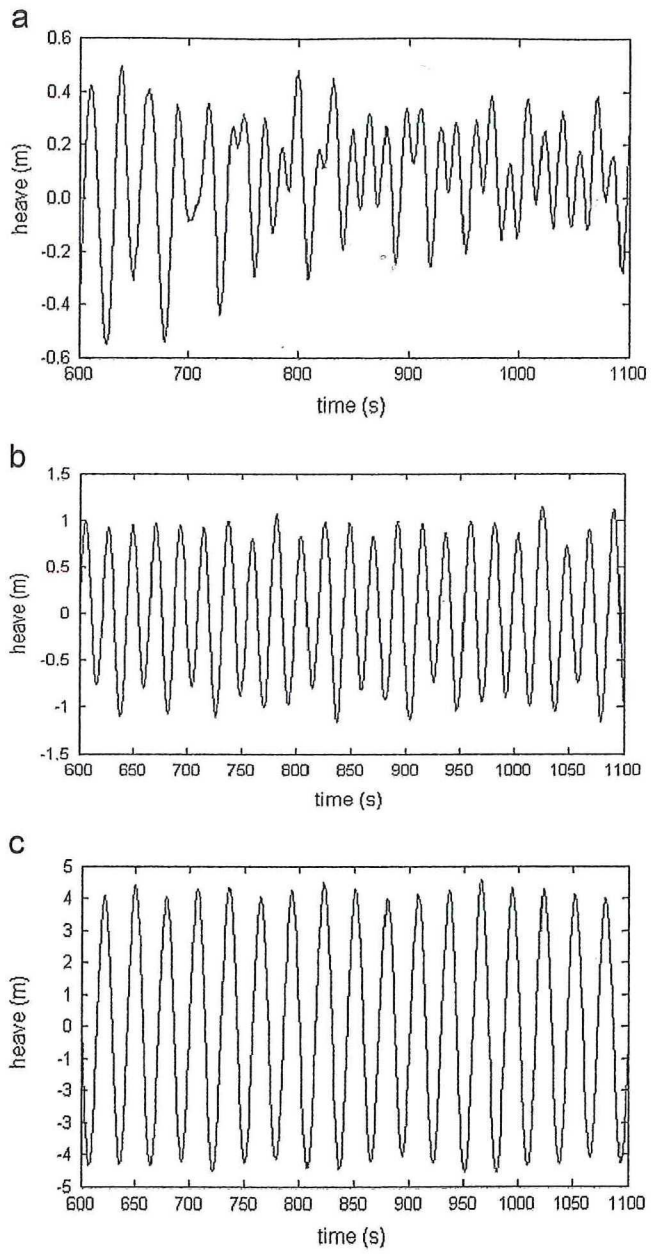

Fig. 24. Platform heave time histories for Case 3, wave height 4 m: (a) wave period 15.5 s, (b) wave period 22.0 s, (c) wave period 28.5 s.

platform due to strong dynamic coupling. Thus coupling of the moon pool water should be considered in the cases of semi-closed moon pool.

(3) The motions of the moon pool are mainly affected by the coupling mass coefficient α_3, hydrodynamic coefficients α_1 and K_g. The influence will be transferred to the heave motions of the platform in cases of larger opening ratio of the moon pool due to the dynamic coupling. The platform heave is mainly affected by the coupling mass coefficient α_4. Hydrodynamic coefficient α_w has little effect on the heave motions of the platform and the motions of the moon pool.

(4) The nonlinear damping is much more enhanced in the cases of semi-closed moon pool. The maximum value of amplitude response curve of the platform heave nonlinearly decreases with the increase of nonlinear damping.

In this paper the nonlinear damping coefficient of platform heave was obtained from the model experiments. It can be calculated by the CFD (computational fluid dynamic) method, this is our research work of next step.

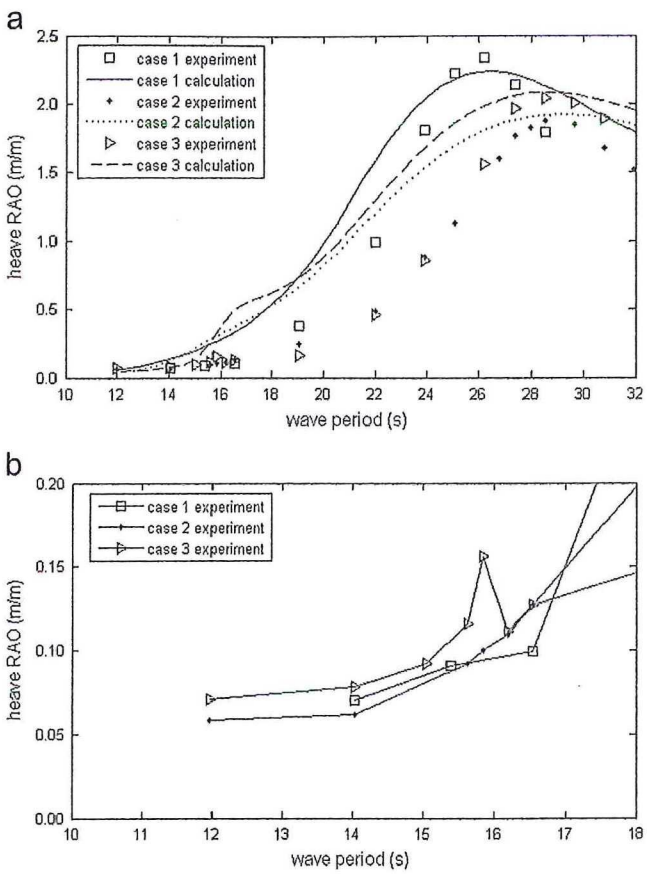

Fig. 25. Response amplitude curves of the platform heave by the experiment: (a) the whole graph, (b) the local magnification graph.

Acknowledgments

The project was supported by the Natural Science Foundation of China under Grant no. 51179125, the Innovation Foundation of Tianjin University under Approving no. 1301 and also supported by China Scholarship Council (CSC).

References

Aalbers, A., 1984. The water motions in a moonpool. Ocean Eng. 11 (6), 557–579.

Barreira, R., Sphaier, S.H., Masetti, I.Q., 2005. Behavior of a mono-column structure (monobr) in waves. In: Proceedings of 24th International Conference on Offshore Mechanics and Arctic Engineering, OMAE2005-67512, Halkidiki, Greece.

Drobyshevski, Y., 2004. Hydrodynamic coefficients of a two-dimensional, truncated rectangular floating structure in shallow water. Ocean Eng. 31 (3-4), 305–341.

Faltinsen, O.M., 1990. Sealoads on Ships and Offshore Structures. Cambridge University Press, Cambridge, UK.

Faltinsen, O.M., Timokha, A.N., 2009. Sloshing. Cambridge University Press, Cambridge, UK.

Ghosh, R., Spanos, Pol D., 2009. Determination of offshore spar stochastic structural response accounting for nonlinear stiffness and radiation damping effects. J. Mech. Mater. Struct. 4 (7-8), 1327–1340.

Gupta, H., Blevins, R., Banon, H., 2008. Effect of moonpool hydrodynamics on spar heave. In: Proceedings of 27th International Conference on Offshore Mechanics and Arctic Engineering, OMAE2008-57264, Estoril, Portugal.

Hansen, A.G., 1967. Fluid Mechanics. John Wiley and Sons, New York, NY.

Jameel Mohammed, Ahmad Suhail, Islam A.B.M. Saiful, Jumaat Mohd Zamin, 2011. Nonlinear analysis of fully coupled integrated Spar-mooring line system. In: Proceedings of the 21st International Offshore and Polar Engineering Conference, Maui, Hawaii, USA.

Kim, M.H., Ran., Z, Zheng., W, 2001. Hull/Mooring coupled dynamic analysis of a truss spar in time domain. Int. J. Offshore Polar Eng. 11 (1), 42–54.
Kristiansen, T., Faltinsen, O.M., 2012. Gap resonance analyzed by a new domain-decomposition method combining potential and viscous flow. Appl. Ocean Res. 34 (1), 198–208.
Li, B.B., Ou, J.P., 2009. Heave response analysis of truss Spar in frequency domain. Ocean Eng. 27 (1), 8–15 (in Chinese).
Liu, L.Q., Zhou, B., Tang, Y.G., 2014. Study on the nonlinear dynamic behavior of deep sea Spar platform by numerical simulation and model experiment. J. Vib. Control 20 (10), 1528–1537.
Lu, Roger R., Wang, Jim J., Ellen Erdal, 2003. Time domain strength and fatigue analysis of truss Spar heave plate. In: Proceedings of the 13th International Offshore and Polar Engineering Conference, Honolulu, Hawaii, USA.
Petter, A.B., 2000. Dynamic Response Analysis of a Truss Spar in Waves. PhD Thesis. Newcastle, University of Newcastle.
Spanos, P.D., Vincenzo Nava, R., Arena, F., 2011. Coupled surge-heave-pitch dynamic modeling of Spar-moonpool-riser interaction. J. Offshore Mech. Arct. Eng. 133 (2) (No.021301).
Sphaier, S.H., Torres, F.G.S., Masetti, I.Q., Costa, A.P., Levi, C., 2007. Monocolumn behavior in waves: experimental analysis. Ocean Eng. 34, 1724–1733.
Tang, Y.G., 2008. Ocean Engineering Structural Dynamics. University Press, Tianjin, Tianjin (in Chinese).
Tao, L.B., Lim, K.Y., Thiagarajan, K., 2004. Heave response of classic Spar with variable geometry. J. Offshore Mech. Arct. Eng. 126 (1), 90–95.
Weggel, D.C., Roesset, J.M., 1994. Vertical hydrodynamic forces on truncated cylinders. In: Proceedings of the Fourth International Offshore and Polar Engineering Conference, Osaka, Japan.
White, F.M., 2003. Fluid MechanicsMcGraw Hill, New York, NY.
Xu, L.X., Jing, X.N., 2013. Calculating riser dynamic effects on Spar motions in waves. In: Proceedings of the 23rd International Offshore and Polar Engineering Conference, Anchorage, Alaska, USA.